Nanoscale Res Lett (2009) 4:1247–1253
DOI 10.1007/s11671-009-9388-5

NANO PERSPECTIVES

Multi-Layered Films Containing a Biomimetic Stimuli-Responsive Recombinant Protein

J. S. Barbosa · R. R. Costa · A. M. Testera · M. Alonso · J. C. Rodríguez-Cabello · J. F. Mano

Received: 1 April 2009 / Accepted: 2 July 2009 / Published online: 16 July 2009

Abstract Electrostatic self-assembly was used to fabricate new smart multi-layer coatings, using a recombinant elastin-like polymer (ELP) and chitosan as the counterion macromolecule. The ELP was bioproduced, purified and its purity and expected molecular weight were assessed. Aggregate size measurements, obtained by light scattering of dissolved ELP, were performed as a function of temperature and pH to assess the smart properties of the polymer. The build-up of multi-layered films containing ELP and chitosan, using a layer-by-layer methodology, was followed by quartz-crystal microbalance with dissipation monitoring. Atomic force microscopy analysis permitted to demonstrate that the topography of the multi-layered films could respond to temperature. This work opens new possibilities for the use of ELPs in the fabrication of biodegradable smart coatings and films, offering new platforms in biotechnology and in the biomedical area.

J. S. Barbosa · R. R. Costa · J. F. Mano (✉)
3B's Research Group-Biomaterials, Biodegradables and Biomimetics, AvePark, Zona Industrial da Gandra, S. Cláudio do Barco, 4806-909 Caldas das Taipas, Guimarães, Portugal
e-mail: jmano@dep.uminho.pt

J. S. Barbosa · R. R. Costa · J. F. Mano
IBB—Institute for Biotechnology and Bioengineering, PT Government Associated Laboratory, Guimarães, Portugal

A. M. Testera · M. Alonso · J. C. Rodríguez-Cabello
G.I.R. Bioforge, Univ. Valladolid, Edificio I+D, Paseo de Belén, 1, 47011 Valladolid, Spain

A. M. Testera · M. Alonso · J. C. Rodríguez-Cabello
Networking Research Center on Bioengineering, Biomaterials and Nanomedicine (CIBER-BBN), Valladolid, Spain

Keywords Elastin-like polymer · Biodegradable polymers · Biomimetic · Smart coatings · Multi-layers · Self-assembling nano-layers · Tissue engineering · Biomaterials · LbL

Introduction

Surface modification techniques have become a key method in the design of materials with specific biological and chemical interactions, creating and optimizing the substrate by alteration of surface functionality or by thin film deposition [1]. The consecutive self-assembly of nanometre-sized layers of multiply charged macromolecules or other objects onto surfaces has been the base of the so-called Layer-by-Layer (LbL) technology, a very interesting technique that permits a highly inexpensive and readily accessible surface modification [2–4].

LbL deposition has been reported as an easy technique, functional on a wide range of surfaces [3, 5]. This method uses the electrostatic attraction between opposite charges as the driving force for the multi-layer build-up [6–8]. During multi-layers formation, a charged substrate is exposed to solutions containing positive or negative polyelectrolytes, so each adsorption leads to the charge inversion of the surface, and multi-layers are stabilised by strong electrostatic forces. The fact that layers exhibit an excess of positive and negative charges allows films to absorb a great variety of compounds such as proteins, which opens the possibility of incorporating specific ligands to keep biological activity and promote specific cell function. Successful protein/polyion multi-layer assembly provides the possibility of organizing proteins in layers and to build up such layers following "molecular architecture" plans [7, 9, 10]. Zhu et al. [9] explored the build-up of multi-layers of polyethyleneimine/

gelatin to construct an extracellular matrix-like multi-layer onto poly (lactic acid) scaffolds. Berthelemy et al. [11] were able to induce a faster differentiation of endothelial progenitor cells into mature endothelial cells after seeding in multi-layer coatings of poly(sodium-4-styrene-sulfonate)/poly(allylamine hydrochloride).

Smart surfaces play an important role in biotechnology and biomaterials area to provide a dynamic control of materials' properties to direct cell function or biomolecules adhesion [12–14]. Smart surfaces are typically obtained by chemical grafting of macromolecules that exhibit a response to external stimuli such as temperature and pH [15–17]. Such substrates have found applications in distinct areas such as the switching of the wettability of surfaces within extreme ranges [18], to control cell adhesion allowing the fabrication of cell sheets [19, 20], tune the release of drugs [21] or even in controlling biomineralization [22].

It is interesting to combine the facile and versatile fabrication of multi-layers with the concept of smart surfaces. Some attempts were presented before typically using synthetic thermo-responsive polymers such as poly(*N*-isopropylacrylamide), PNIPAAm [23–26].

Elastin-like polymers (ELPs) represent another interesting kind of stimuli-responsive biomimetic macromolecules. Their basic structure is a repeating sequence with its origin in the elastin, an extracellular matrix protein [27–29]. Advances in genetic engineering allow the design and bioproduction of protein-based polymers, following a bottom-up strategy, incorporating selected aminoacid sequences in the molecule structure [29, 30]. The advantage of using such technique resides in the versatility to include peptide domains with the ability to control aspects such as degradability, cell adhesion or biomineralization. Mechanical performance of ELPs is accompanied by an extraordinary biocompatibility, presenting an outstanding acute, smart and self-assembling nature, based on the molecular transition of the polymer chain, in the presence of water, when their temperature is raised above a certain level. This "inverse temperature transition" (ITT) became a key issue in the development of new peptide-based polymers as materials and molecular machines [28, 31].

This work hypothesizes that ELPs may be used to construct multi-nano-layers onto substrates in order to produce biomimetic smart coatings or films without the need of covalent bonds and with a good control of its thickness. Chitosan will be used as the counterion macromolecule for the proof of concept. The use of such biopolymers may also provide a biodegradable character to the multi-layer.

Chitosan is a natural polymer obtained by chitin's partial deacetylation and soluble in aqueous acidic media (pH < 6) due to the protonation of amines, converting the polysaccharide to a polyelectrolyte. This parameter influences chitosan's properties such as solubility, viscosity, crystallinity, reactivity and biodegradability [32–34]. It has widely been used for biomedical applications due to its biological and chemical similarities to natural tissues and its unique biological properties such as biocompatibility, biodegradability to undamaging products, non-toxicity, physiological inertness and remarkable affinity to proteins [32–35].

Materials and Methods

Cloning and molecular biology procedures were performed according to Girotti et al. [36], and sequence of all putative inserts was verified by automated DNA sequencing. A synthetic DNA duplex encoding the oligopeptide [(VPG IG)$_2$ (VPGKG) (VPGIG)$_2$]$_2$ DDDEEKFLRRIGRFG [(VPG IG)$_2$ (VPGKG) (VPGIG)$_2$]$_2$ was generated by polymerase chain reaction (PCR) amplification using synthetic oligonucleotides (IBA GmbH, Goettingen, Germany). The gene cloning, concatenation and colony screening were performed as described in [36].

Expression conditions and purification protocols of the ELP produced in this work, labelled "HAP", were adapted from Mcpherson et al. [37] and Girotti et al. [36]. Terrific Broth medium (TB), with 0.1% carbenicillin and 0.1% glucose, was used for the gene expression under controlled temperature (37 °C). Culture growth of *E. coli* was controlled by registration of optical density variation, at 600 nm (OD600), stopping fermentation when registered an OD600 around 7. After fermentation, centrifuged bacteria were resuspended and lysed by ultrasonic disruption. The obtained lysate went by alternate cold and warm centrifugation cycles. In order to retrieve purified bioproduced polymer, solution was frozen at −24 °C and freeze-dried. During purification steps, sodium chloride (NaCl) was added to a concentration of 0.5 M.

Purity Assessment

Sodium dodecyl sulphate polyacrylamide gel electrophoresis (SDS–PAGE) was performed to assess HAP purity. A polyacrylamide gel was loaded with 5 μL of a HAP solution at 1 mg mL^{-1}. Identification of a major band around 32 kDa was expected, due to the theoretical molecular weight of polymer. A matrix-assisted laser desorption/ionization time-of-flight (MALDI-TOF) mass spectroscopy was also performed to confirm polymer purity degree and polymer molecular weight. The test was performed in a Voyager STR, from Applied Biosystems in linear mode and with an external calibration using bovine serum albumin (BSA).

Temperature Responsiveness

DSC experiments were performed on a Mettler Toledo 822e with liquid nitrogen cooler. For DSC analysis, a solution of HAP, at a concentration of 50 mg mL^{-1}, was prepared in pure water, and its pH was adjusted. For each run, 20 μL of solution were dispensed in a standard 40 μL aluminium pan hermetically sealed. The same volume of water was used as reference. Samples were heated at a rate of 5 °C min^{-1} after being maintained at 5 °C for 5 min. The temperature and heat flow were calibrated using Indium standards at the same operational conditions.

Size Measurement

HAP aggregate size was measured in a Nano-ZS from Malvern, at temperatures ranging from 20 to 40 °C, after 5 min of temperature stabilization. Samples were prepared at 1 mg mL^{-1}, in a solution of NaCl 0.15 M and pH = 5. For each sample, 5 measurements were performed, 12 runs each, in order to obtain the final value for the aggregate size for each temperature step.

Multi-layer Build-up

Purified medium molecular weight chitosan (cht) with a final deacetylation degree of 93.5% (Sigma, ref.448877) and bioproduced HAP were solubilized at 1 mg mL^{-1} in NaCl 0.15 M. Each solution had its pH adjusted to 5. At this pH, amino groups from chitosan are protonated, representing a positively charged polyelectrolyte. HAP, due to the various charged residues, is simultaneously positively and negatively charged, subsequently multi-layer build-up will use negative charges.

A Q-Sense E4 quartz-crystal microbalance with dissipation monitoring (QCM-D) system was the equipment used for monitorization of multi-layer build-up on gold-coated crystals. Crystals went by a clean up procedure in an ultrasound bath at 30 °C while immersed, separately, in acetone, ethanol and isopropanol. Multi-layer formation was measured at room temperature and at a constant flow rate of 50 μL min^{-1}. Firstly, a baseline was made by priming the system with a 0.15 M NaCl solution during 15 minutes. Then, deposition of chitosan and HAP was made, pumping solutions into the system for 10 minutes, where each deposition was followed by a rinsing step with a NaCl 0.15 M solution, for the same time. Real time monitorization was made for Δf and ΔD. An AT cut quartz crystal is excited at a fundamental frequency, about 5 MHz, as well as at the 3rd, 5th, 7th, 9th, 11th and 13th overtones.

For the preparation of multi-layer coatings, regular microscopy glass slides were cut into small pieces (7 × 7 mm^2) and went through the same cleaning procedure of the QCM-D crystals. The same protocol used on the QCM experiments was followed, dipping glass slides in similar solutions, in order to obtain the multi-layer coatings. Samples were prepared in order to obtain 5 pairs of bilayers, being the last composed of HAP, designated $(Cht\text{-}HAP)_5$, and samples terminated by chitosan designated $(Cht\text{-}HAP)_4Cht$.

Surface Characterization

Atomic force microscopy (AFM) measurements were performed in a MultiMode STM microscope controlled by the NanoScope III from Digital Instruments system, operating in tapping mode at a frequency of 1 Hz with RTESP tips and an amplitude of 1.5–2 V. The coated glass slides were immersed in a 0.15 M NaCl solution for 30 min prior to measurement to hydrate the polyelectrolyte layers. To assess temperature response of the coatings, the samples were immersed in saline solution at room temperature and above T_t, separately. The analysed area was 10 × 10 μm^2. For the AFM analysis, samples were retrieved from the solution.

Results and Discussion

The elastin-like polymer used in this work, designated HAP, containing an osteoconductive sequence, was obtained by bioproduction of genetically modified *E. coli*.—see Materials and methods. After purification, both SDS–PAGE and MALDI-TOF tests were performed to verify both the molecular weight and the purity of the obtained polymer, respectively. Results are shown in Fig. 1.

ELPs in aqueous solution and below the transition temperature (T_t) are solubilized and, above it, the chains aggregate into larger structures. This behaviour was used during the purification process in order to retrieve the purified polymer by cold and warm centrifugation cycles. The designed biopolymer has a theoretical molecular weight of 31,877 Da. The results obtained from electrophoresis (intense band in Fig. 1a) and MALDI-TOF (sharp peak in Fig. 1b) show the correctness of the sequence length, as well as the desired composition of the polymer.

HAP is a recombinant ELP that possesses many positively and negatively charged residues. Therefore, T_t is expected to depend on pH; DSC scans were performed at different pH values to investigate the phase transition of HAP in solution. T_t and ITT enthalpy (ΔH), obtained from the endothermic event observed during heating, are represented in Fig. 2a for a pH ranging from 4 to 12.

The DSC results suggest a general decrease in T_t as the pH increases. This fact is due to the protonation state of free lysines, present in the biopolymer chain, that possess

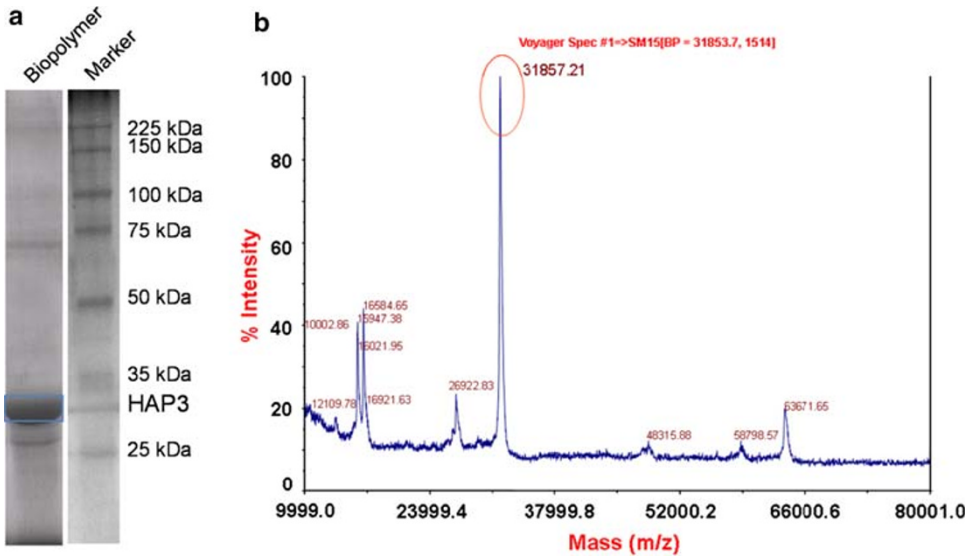

Fig. 1 Polymer's purity and molecular weight assessments: **a** SDS–PAGE and **b** MALDI-TOF

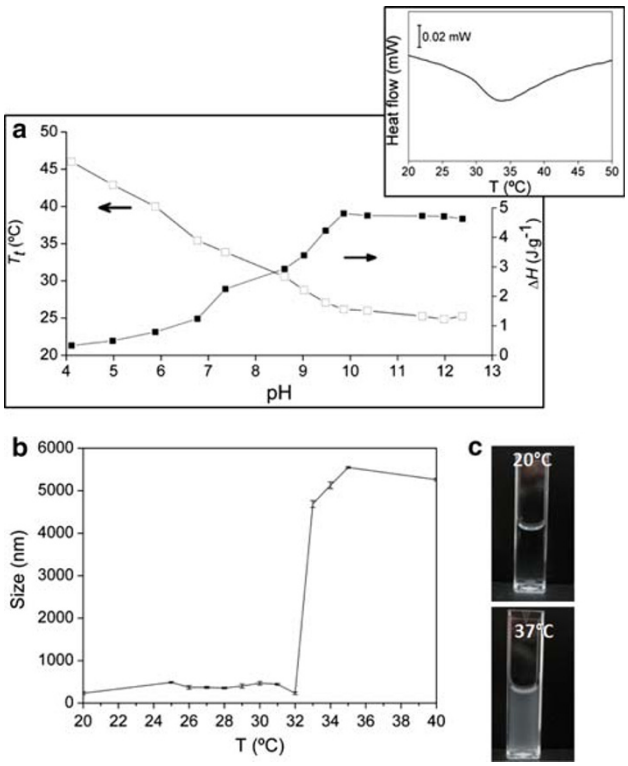

Fig. 2 **a** Transition temperature (□) and enthalpy (■) obtained from DSC scans; inset represents DSC curve for pH = 7.36; **b** aggregation size profile obtained from size measurement and **c** turbidity change of the solution used for size determination

free amino groups and a pKa around 10.6. For pH under this value, amino groups are protonated presenting a cationic behaviour while at pH above their pKa amines become deprotonated and hydrophobic interactions are dominant. As referred in the literature, the more apolar the ELP, the lower the T_t [29]. It is interesting to note that at physiological pH (as shown on the inset of Fig. 2a), the ITT of the polymer is around 34 °C that makes the material potentially interesting for biomedical applications such as drug delivery systems, as smart surfaces or hydrogels for tunable adhesion of cells or proteins.

The DSC data also show that the enthalpy of the transition increases as pH increases. Two phenomena contribute for the total enthalpy: the ordering of biopolymer chain into the β-spiral structure, corresponding to a reversing exothermic event, and the destruction of the ordered hydrophobic hydration structures around the polymer chain, which represent a non-reversing endothermic event [29, 38]. The endothermic process contributes with more than three times than the exothermic component for the total enthalpy. The more hydrophobic is the polymer, the higher is the registered ΔH due to the increasing in water molecules dedicated to hydrophobic hydration. The higher the pH, the more hydrophobic the ELP becomes and, consequently, the higher the ΔH values. The addition of salt to the solution facilitates self-assembly of the polymer due to a variation on the electrostatic interactions, decreasing the T_t and increasing ΔH, when compared with the same conditions in pure water (results not shown).

The aggregation size was also studied and the obtained results are shown in Fig. 2b as a function of temperature. It is possible to observe an abrupt increase in the aggregate size that varies from around 250 nm at 32 °C to 4,700 nm at 33 °C, which represents the T_t of the biopolymer for the studied conditions. This aggregation is due to the change in the conformation of polymer chains imposed by the hydrophobic association of the polymer free side chains: below T_t, chains adopt a free random-coil conformation but above T_t, chains collapse and aggregate into micron-sized structures. In Fig. 2c, it is possible to observe the turbidity change in HAP solution with the increase in temperature. This increase in the solution turbidity is due to the

aggregation of polymer chains above T_t, which causes the segregation of the ELP from the solution.

It would be interesting to verify if such kind of smart elastin-like polymers could be used to produce multi-layered films with a biopolymer such as chitosan. The occurrence of charged sequences along its structure provides an indication that such coatings may be formed through electrostatic interactions.

The multi-layer build-up of chitosan and HAP was studied by monitoring its adsorption to surface of gold-coated crystals using QCM-D. The sensitivity of this method permits to detect adsorption of small amounts of material on the surface and allows to characterize the viscoelastic properties of the formed film. Crystal resonance frequency depends on total oscillating mass, including the solution coupled to the oscillation, decreasing when a thin film is formed in the sensor crystal. Moreover, it is also possible to detect dissipating energy, due to the fact that adsorbed films are not rigid, exhibiting a viscoelastic behaviour [39, 40]. In Fig. 3, the changes in frequency (Δf) and dissipation (ΔD) of 5th, 7th and 9th overtones, during multi-layers' construction, are represented.

Figure 3a and b present the deposition and rinsing cycles of chitosan and HAP. In each deposition step, there is a reduction on the frequency corresponding to the deposition of polymer in the crystal's surface and a smaller increase in Δf during the rinsing steps that corresponds to the removal of some material that is not adhered on the surface (Fig. 3a). The flattening of the frequency curves at the end of each rinsing step indicates that remaining polymer mass is stable enough not to be removed, indicating a stable polyelectrolyte film formation.

The increase in ΔD during the deposition of chitosan indicates the formation of a more viscoelastic film (Fig. 3b). However, it is interesting to notice that the deposition of HAP has an opposite effect, stiffening the films' surface. The net behaviour upon consecutive depositions is for a progressive formation of a more viscoelastic film with greater dampening characteristics. The QCM-D results evidence the possibility of using such polymers in order to obtain stable multi-layer films over surfaces.

More insights can be obtained by modelling the QCM-D data. The Voigt viscoelastic model [41] was used to extract the change in the film thickness during the polymer deposition. Figure 3c shows the results obtained for the change in the thickness upon individual layer formation. The deposition of chitosan onto a HAP-terminated multi-layer contributes for an increase in about 6 nm for the total thickness. This increment seems to decrease slightly, however, appears to be almost independent on the number of multi-layers. Surprisingly, when HAP is added the thickness of the multi-layer decreases by values around 2 nm. This decrease, however, is smaller for higher number

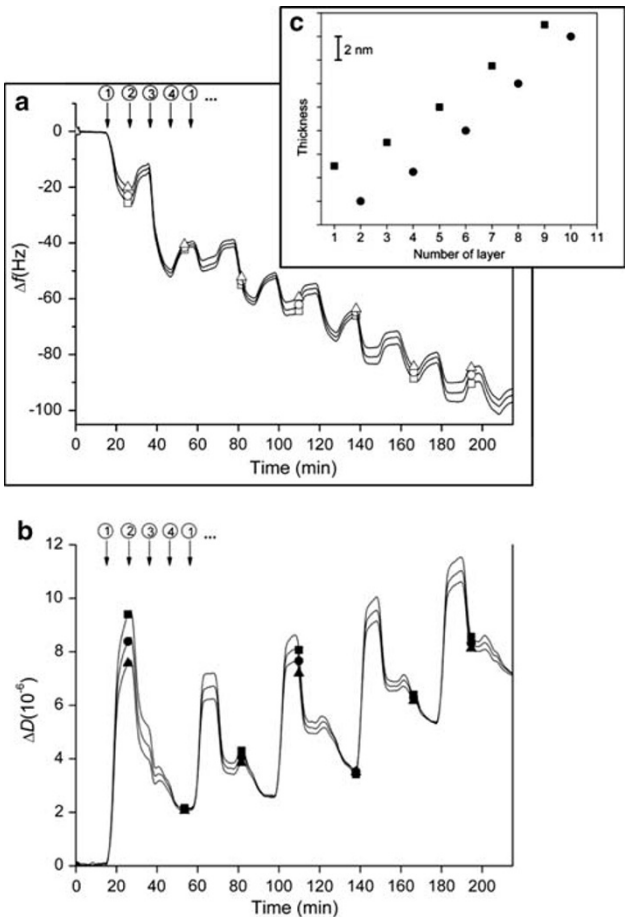

Fig. 3 **a** Frequency changes during LbL chitosan-HAP build-up: 1-Cht deposition, 2-rinsing, 3-H AP deposition and 4-rinsing. **b** Dissipation changes during LbL chitosan-HAP build-up: 1-Cht deposition, 2-rinsing, 3-H AP deposition, and 4-rinsing. The 5th (*squares*), 7th (*circles*) and 9th (*triangles*) overtones are represented. **c** Change in the film's thickness during LbL build-up: cht (*squares*) and HAP (*circles*)

of layers. A possible explanation for this behaviour could be the strong interaction of such polymer with chitosan, leading to a partial dehydration of the terminal layer and a change of the macromolecular conformations towards a more extended shape. Such hypothesis is in accordance with the decrease in the dissipation energy values upon HAP deposition (Fig. 3b).

It would be interesting to verify whether the change in chain conformation and aggregation ability found in HAP in solution could be transposed to the multi-layered films obtained with chitosan. We hypothesize that the modifications in the polymeric chains organization, associated with the ITT, could influence the topography of the surface.

The characterization of polyelectrolyte surfaces was made by AFM. After preparation of multi-layer samples, slides were placed in saline solutions under and above T_t. Results obtained for the topography analysis are shown in Fig. 4.

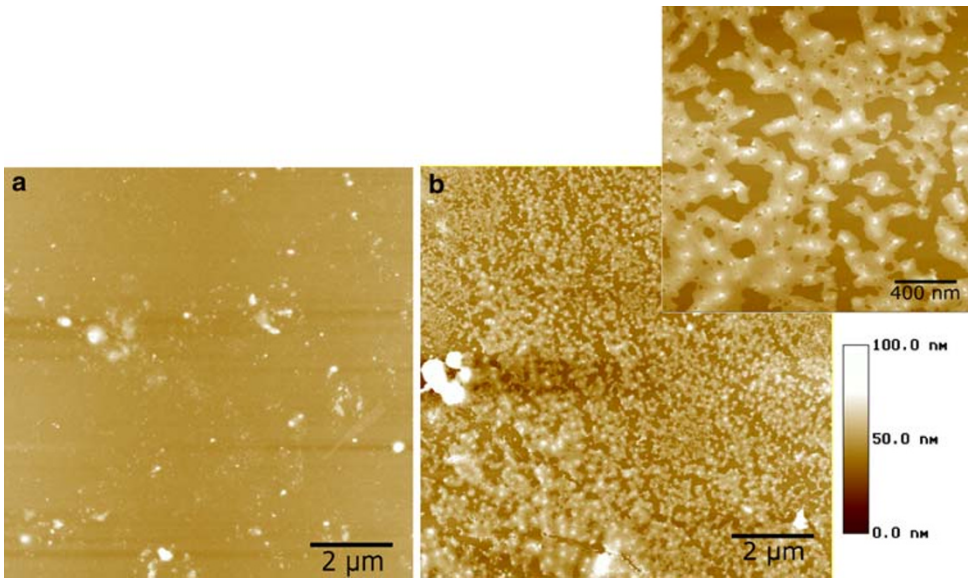

Fig. 4 AFM surface characterization: **a** $(Cht\text{-}HAP)_5$ under T_t and **b** $(Cht\text{-}HAP)_5$ above T_t (two magnifications)

It is possible to observe from the AFM images that the biopolymer HAP shows a responsive behaviour across its ITT even when it is assembled in the multi-layers with chitosan. In fact, the $(Cht\text{-}HAP)_5$ below T_t exhibits a quite smooth surface (Fig. 4a) but above the ITT clear nano-sized agglomerates can be seen, which may result from the collapse of adjacent HAP chains in the surface (Fig. 4b). It should be mentioned that such nano-structures are almost absent if the multi-layers are ended with the polysaccharide (results not shown). The aggregate sizes in the surface (inset of Fig. 4b) are much smaller than the ones formed in solution (Fig. 2b). This may be explained by the fact that, in solution, the association and aggregation of polymer chains is much more facilitated than when the polymer is attached in the surface after deposition over chitosan layers.

Conclusion

An elastin-like polymer was produced, purified and its responses to temperature and pH were investigated. We successfully demonstrated that this biomimetic polymer could be used in the build-up of self-assembled multi-layers with chitosan. It has been shown that the temperature-responsive behaviour, originally presented by the biopolymer, is present in the modified surfaces having HAP as the outermost layer. This work opens new possibilities for the use of elastin-like polymers in the fabrication of coatings and films with stimuli-responsive behaviour, offering new platforms in biotechnology and in the biomedical area.

Acknowledgments This work was supported by the Fundação para a Ciência e Tecnologia (Portugal) under project PTDC/QUI/68804/2006. This work was also supported by the Fundação para a Ciência e Tecnologia (Portugal) under projects PTDC/FIS/61621/2004, PTDC/QUI/68804/2006 and PTDC/QUI/69263/2006. The work performed in Valladolid was supported by the "Junta de Castilla y Leon" (VA087A06, VA016B08 and VA030A08), by the MEC (MAT2007-66275-C02-01 and NAN2004-08538), by the Marie Curie RTN Biopolysurf (MRTN-CN-2004-005516) and by the European Commission for the Erasmus Programme.

References

1. R.N.S.J. Sodhi, Electron Spectrosc. Relat. Phenom. **81**, 269–284 (1996)
2. G. Decher, Science **277**, 1232–1237 (1997)
3. P.T. Hammond, Curr. Opin. Colloid Interface Sci. **4**, 430–442 (1999)
4. C. Picart, P. Lavalle, P. Hubert, F.J.G. Cuisinier, G. Decher, P. Schaaf, J.C. Voegel, Langmuir **17**, 7414–7424 (2001)
5. Z.Y. Tang, Y. Wang, P. Podsiadlo, N.A. Kotov, Adv. Mater. **18**, 3203–3224 (2006)
6. Y. Lvov, H. Haas, G. Decher, H. Mohwald, A. Kalachev, J. Phys. Chem. **97**, 12835–12841 (1993)
7. H.G. Zhu, J. Ji, J.C. Shen, Biomacromolecules **5**, 1933–1939 (2004)
8. C. Picart, J. Mutterer, L. Richert, Y. Luo, G.D. Prestwich, P. Schaaf, J.C. Voegel, P. Lavalle, Proc. Natl. Acad. Sci. USA **99**, 12531–12535 (2002)
9. H.G. Zhu, J. Ji, Q.G. Tan, M.A. Barbosa, J.C. Shen, Biomacromolecules **4**, 378–386 (2003)
10. T.I. Croll, A.J. O'Connor, G.W. Stevens, J.J. Cooper-White, Biomacromolecules **7**, 1610–1622 (2006)
11. N. Berthelemy, H. Kerdjoudj, C. Gaucher, P. Schaaf, J.F. Stolz, P. Lacolley, J.C. Voegel, P. Menu, Adv. Mater. **20**, 2674–2678 (2008)
12. M. Yoshida, R. Langer, A. Lendlein, J. Lahann, Polym. Rev. **46**, 347–375 (2006)
13. K.F. Ren, T. Crouzier, C. Roy, C. Picart, Adv. Funct. Mater. **18**, 1378–1389 (2008)
14. C. Picart, Curr. Med. Chem. **15**, 685–697 (2008)
15. J.F. Mano, Adv. Eng. Mater. **10**, 515–527 (2008)
16. Y. Ikada, Biomaterials **15**, 725–736 (1994)

17. P.M. Mendes, Chem. Soc. Rev. **37**, 2512–2529 (2008)
18. F. Xia, H. Ge, Y. Hou, T. Sun, T.L. Sun, L. Chen, G.Z. Zhang, L. Jiang, Adv. Mater. **19**, 2520–2524 (2007)
19. H. Hatakeyama, A. Kikuchi, M. Yamato, T. Okano, Biomaterials **27**, 5069–5078 (2006)
20. R.M.P. Da Silva, J.F. Mano, R.L. Reis, Trends Biotechnol. **25**, 577–583 (2007)
21. D. Volodkin, Y. Arntz, P. Schaaf, H. Moehwald, J.C. Voegel, V. Ball, Soft Matter **4**, 122–130 (2008)
22. J. Shi, N.M. Alves, J.F. Mano, Adv. Func. Mater. **17**, 3312–3318 (2007)
23. J.E. Wong, A.K. Gaharwar, D. Muller-Schulte, D. Bahadur, W. Richtering, J. Colloid Interf. Sci. **324**, 47–54 (2008)
24. S.A. Sukhishvili, Curr. Opin. Colloid Interface Sci. **10**, 37–44 (2005)
25. K. Glinel, C. Dejugnat, M. Prevot, B. Scholer, M. Schonhoff, R.V. Klitzing, Colloid Surf. A-Physicochem. Eng. Asp **303**, 3–13 (2007)
26. M. Prevot, C. Dejugnat, H. Mohwald, G.B. Sukhorukov, ChemPhysChem **7**, 2497–2502 (2006)
27. M. Haider, Z. Megeed, H. Ghandehari, J. Control Release **95**, 1–26 (2004)
28. D.W. Urry, T.M. Parker, M.C. Reid, D.C. Gowda, J. Bioact. Compat. Polym. **6**, 263–282 (1991)
29. J.C. Rodríguez-Cabello, J. Reguera, A. Girotti, F.J. Arias, M. Alonso, Adv. Polym. Sci. **200**, 119–167 (2006)
30. J.C. Rodriguez-Cabello, Smart elastin-like polymers. In *Biomaterials: from Molecules to Engineered Tissues*, ed. by N. Hasirci, V. Hasirci (Kluwer Academic/Plenum Publ, New York, 2004), pp. 45–57
31. F.J. Arias, V. Reboto, S. Martin, I. Lopez, J.C. Rodriguez-Cabello, Biotechnol. Lett. **28**, 687–695 (2006)
32. M. Rinaudo, Prog. Polym. Sci. **31**, 603–632 (2006)
33. I.Y. Kim, S.J. Seo, H. Moon, M.K. Yoo, I.Y. Park, B.C. Kim, C.S. Cho, Biotechnol. Adv. **26**, 1–21 (2008)
34. A. Di Martino, M. Sittinger, M.V. Risbud, Biomaterials **26**, 5983–5990 (2005)
35. N.M. Alves, J.F. Mano, Int. J. Biol. Macromol. **43**, 401–414 (2008)
36. A. Girotti, J. Reguera, F.J. Arias, M. Alonso, A.M. Testera, J.C. Rodríguez-Cabello, Macromolecules **37**, 3396–3400 (2004)
37. D.T. Mcpherson, C. Morrow, D.S. Minehan, J.G. Wu, E. Hunter, D.W. Urry, Biotechnol. Prog. **8**, 347–352 (1992)
38. J.C. Rodriguez-Cabello, J. Reguera, M. Alonso, T.M. Parker, D. McPherson, D.W. Urry, Chem. Phys. Lett. **388**, 127–131 (2004)
39. E.J. Park, D.D. Draper, N.T. Flynn, Langmuir **23**, 7083–7089 (2007)
40. S.M. Notley, M. Eriksson, L. Wagberg, J. Colloid Interface Sci. **292**, 29–37 (2005)
41. M.V. Voinova, M. Rodahl, M. Jonson, B. Kasemo, Phys. Scr. **59**, 391–396 (1999)